

AD _____

Award Number: W81XWH-10-1-0626

TITLE: Placental Vascular Tree as Biomarker of Autism/ASD Risk

PRINCIPAL INVESTIGATOR: Carolyn M. Salafia, M.S., M.D.

CONTRACTING ORGANIZATION: Research Foundation for Mental Hygiene
Staten Island, NY 10314

REPORT DATE: September 2011

TYPE OF REPORT: Annual

PREPARED FOR: U.S. Army Medical Research and Materiel Command
Fort Detrick, Maryland 21702-5012

DISTRIBUTION STATEMENT: Approved for Public Release;
Distribution Unlimited

The views, opinions and/or findings contained in this report are those of the author(s) and should not be construed as an official Department of the Army position, policy or decision unless so designated by other documentation.

| REPORT DOCUMENTATION PAGE | | | <i>Form Approved</i> <i>OMB No. 0704-0188</i> | | |
|--|-------------------------|---------------------------------|--|--|---|
| Public reporting burden for this collection of information is estimated to average 1 hour per response, including the time for reviewing instructions, searching existing data sources, gathering and maintaining the data needed, and completing and reviewing this collection of information. Send comments regarding this burden estimate or any other aspect of this collection of information, including suggestions for reducing this burden to Department of Defense, Washington Headquarters Services, Directorate for Information Operations and Reports (0704-0188), 1215 Jefferson Davis Highway, Suite 1204, Arlington, VA 22202-4302. Respondents should be aware that notwithstanding any other provision of law, no person shall be subject to any penalty for failing to comply with a collection of information if it does not display a currently valid OMB control number. PLEASE DO NOT RETURN YOUR FORM TO THE ABOVE ADDRESS. | | | | | |
| 1. REPORT DATE September 2011 | | 2. REPORT TYPE Annual | | 3. DATES COVERED 15 August 2010 – 14 August 2011 | |
| 4. TITLE AND SUBTITLE Placental Vascular Tree as Biomarker of Autism/ASD Risk | | | 5a. CONTRACT NUMBER | | |
| | | | 5b. GRANT NUMBER W81XWH-10-1-0626 | | |
| | | | 5c. PROGRAM ELEMENT NUMBER | | |
| 6. AUTHOR(S) Carolyn M. Salafia, M.S., M.D. E-Mail: carolyn.salafia@gmail.com | | | 5d. PROJECT NUMBER | | |
| | | | 5e. TASK NUMBER | | |
| | | | 5f. WORK UNIT NUMBER | | |
| 7. PERFORMING ORGANIZATION NAME(S) AND ADDRESS(ES) Research Foundation for Mental Hygiene Staten Island, NY 10314 | | | 8. PERFORMING ORGANIZATION REPORT NUMBER | | |
| 9. SPONSORING / MONITORING AGENCY NAME(S) AND ADDRESS(ES) U.S. Army Medical Research and Materiel Command Fort Detrick, Maryland 21702-5012 | | | 10. SPONSOR/MONITOR'S ACRONYM(S) | | |
| | | | 11. SPONSOR/MONITOR'S REPORT NUMBER(S) | | |
| 12. DISTRIBUTION / AVAILABILITY STATEMENT Approved for Public Release; Distribution Unlimited | | | | | |
| 13. SUPPLEMENTARY NOTES | | | | | |
| 14. ABSTRACT We propose to capitalize on recent insights into the shared molecular pathways that support and maintain neuronal and vascular branching growth and an internationally unique resource, the ALSPAC longitudinal birth cohort with immaculately preserved placentas, to test the idea that appropriate measures of the shape and structure of the branching network of the placental vascular tree that is progressively elaborated across gestation will serve as biomarkers of autism/ASD and provide a novel method of assessment of the placental vascular tree. To validate the theory that placental vascular tree structure serves as a biomarker of autism/ASD risk, we are proposing one task—the examination, dissection, and photography of the study placentas—and three subprojects which will use the images and other data gathered from that processing to characterize the shape and structure of the placental vascular trees and the gestational environments of children diagnosed with autism/ASD compared to a comprehensive set of two control groups. The placental examination and dissection, and the subprojects will be drawn from a nested case control study of the placental archive of the Avon Longitudinal Study of Parents and Children (ALSPAC). The case group will include all 56 children in the cohort with archived placentas who have been diagnosed with autism/ASD. Two control groups of 168 placentas/children each (3:1 ratio to cases) will be selected from the same cohort: 1. One control group will be drawn from the cohort members (n > 6500) with normal childhood development. 2. The second control group will consist of cohort members without autism/ ASD but diagnosed with developmental delay and requiring special education needs (SEN). Each control group will be frequency-matched to the autism case group on the following three variables: gender; gestational age category, and parity. (Total sample size: 371 placentas). Maternal medical record data have been extracted for all children. | | | | | |
| 15. SUBJECT TERMS Autism | | | | | |
| 16. SECURITY CLASSIFICATION OF: | | | 17. LIMITATION OF ABSTRACT | 18. NUMBER OF PAGES | 19a. NAME OF RESPONSIBLE PERSON USAMRMC |
| a. REPORT U | b. ABSTRACT U | c. THIS PAGE U | | | |

Table of Contents

| | <u>Page</u> |
|--|-------------|
| Introduction..... | 1 |
| Body..... | 2 |
| Key Research Accomplishments..... | 14 |
| Reportable Outcomes..... | 15 |
| Conclusion..... | 16 |
| References..... | 17 |
| Appendices..... | 18 |

Annual Report Year #1**September 13, 2011****Program Project Title:**

Characterization of the Placental Vascular Tree as a Biomarker of Autism/ASD Risk

Program Project PI: Carolyn M. Salafia MD, MS**INTRODUCTION**

The overall aim of this multidisciplinary program project is to determine the correlation between patterns of placental branching growth at all levels of the placental vascular tree with diagnosis of autism/ASD as compared to diagnoses of special education needs (SEN) and “normal” outcomes, and to develop a risk assessment tool built on measures of placental shape and structure that can be performed on all infants at birth to improve identification of children who are at increased risk of autism/ASD for their early screening and diagnosis.

In this project we will measure the branching of larger blood vessels on the surface of the placenta (2D), the placental shape (that contains the placental vascular fractal), and the branching structure of the fine vessels of the thickness of the placenta (3D), and analyze the maternal medical and gestational factors that may have led to differences observed between the autism/ASD group, a group of children with other special educational needs and healthy control children.

The placental examination and dissection, and the subprojects will be drawn from a nested case control study of the placental archive of the Avon Longitudinal Study of Parents and Children (ALSPAC). The proposed case group included all 56 children in the cohort with archived placentas who have been diagnosed with autism/ASD. Two control groups of children were available from the same cohort, one with special education needs (SEN) but not a diagnosis of autism/ASD, and one with no diagnoses related to neurodevelopmental pathology, at a 3:1 ratio to cases.

Our findings thus far include:

1. There was a statistically significant reduction in placental weight (~100 g) for female autism/ASD cases compared to female normal controls. There is also a significant difference in beta, a measure of the integrity of the placental vascular fractal in autism/ASD cases compared to female normal controls.). By contrast, β did differ by gestational age in boys. Gestational age may act through changes in beta to influence autism/ASD risk. These observations are independent of any effect of gestational age.
2. Analyses of the 2D images show that umbilical cord marginality - defined either by the first Fourier coefficient or more directly as the distance from the cord insertion to the disk edge - differs significantly between autism/ASD cases and the University of North Carolina Pregnancy, Infection and Nutrition Study (UNC PIN) birth cohort.

These support our hypothesis that placental growth patterns are altered in autism/ASD and will focus our analyses next year to determine the optimal measurement tools for autism/ASD risk assessment in the delivered placenta.

BODY

Autism/ASD reflects a range of disordered and impaired brain development which leads to a lifelong course of behavioral and cognitive abnormalities. Diagnosis cannot formally be made prior to age two and this point there is a lack of behavioral and biologic markers that we can use to predict its onset. Early predictors could lead to early interventions which might significantly improve the lives of those affected. We intend to use the fact that the same biochemistry that controls the branching of nerves also controls branching of blood vessels. Unlike the nerve networks in the living human brain, the branching of the blood vessels in a child's placenta (that is generally discarded after birth without any examination) can be photographed and dissected. Our methods have expressly focused on capture of potentially key placental vascular features using equipment and procedures that could be performed at any hospital delivering a baby in the US. Thus, if successful, our work could lead to the routine examinations of placentas at birth to provide a noninvasive newborn screening test to identify children at high risk for developing autism/ASD.

In this project we will measure the branching of larger blood vessels on the surface of the placenta (2D), the placental shape (that contains the placental vascular fractal), and the branching structure of the fine vessels of the thickness of the placenta (3D), and analyze the maternal medical and gestational factors that may have led to differences observed between the autism/ASD group, a group of children with other special educational needs and healthy control children. We have developed and will apply new tools to analyze digital images of placental blood vessel branching, and the mathematics required to analyze the complex patterns of this placental branching architecture. In addition to its use as a biomarker, the application of these techniques has the potential to both clarify the pathologic anatomy of autism/ASD, and to determine when during pregnancy autism/ASD might have developed.

Any model generated in a single population will require validation prior to its general use in public health screening. Collection of a new cohort, and confirmation of positive results from this study have generated preliminary data in families with an autistic child (in placentas of subsequently delivered infants who will begin to be able to be evaluated for autism within the next 6 months. Thus this research is being applied in current studies of high-autism risk siblings (E.A.R.L.I., PI: Craig Newschaffer, PhD) and M.A.R.B.L.E.S. (PI: Cheryl Walker, MD) networks, and shows early promise of being able to rapidly contribute to our understanding of likely pathways of disordered neurodevelopment in this highly heterogeneous spectrum of autism/ASD.

Task: Placental processing: *P.I.: Carolyn M Salafia, MD, NYS Institute for Basic Research in Developmental Disabilities (IBR), 1050 Forest Hill Road, Staten Island, NY, 10314. Co-Investigators: Dr Craig Charles Platt, Consultant Perinatal Pathologist and Ms Roisin Armstrong University Hospitals Bristol NHS Foundation Trust and Professor Jean Golding, Sue Ring, PhD, Mr Colin Steer, Ms Amanda Carmichael, ALSPAC, University of Bristol, Bristol, UK (no animal or human use at any of the above addresses except for use of archived anonymized placental specimens only at ALSPAC).*

The specified placentas will be photographed and grossly processed according to protocols that Dr. Salafia previously implemented successfully in a birth cohort, and upon which placental protocols for the U.S. National Children's Study are based. These protocols will yield chorionic surface photographs that image the 2-D chorionic surface vascular tree, and serially blocked regions of the placental parenchyma from which serial sections of histologic slides can be digitized to reconstruct the 3-D (finer) chorionic vascular branched tree.

Timeline: *The 392 placentas will be fully examined, dissected and tissues processed in the first 3 months of Year 1.*

Status: *The placental sample size now totals 53 autism/ASD cases, 145 non-ASD/non-SEN controls, and 150 SEN controls. The reasons for the sample size change from the original proposal is 3(~5%) of the mothers with children subsequently diagnosed with autism/ASD had not given consent for the placentas to be part of subsequent research protocols. A higher percentage of the SEN controls (~ 10%) and normal (non-ASD/non-SEN) controls (~13%) and had also not provided consent. Thus a total of 53 cases*

plus 18 special education needs controls matched controls and 23 non-ASD/ non-SEN controls were also not included in the sample of placentas for analysis.

The protocol included obtaining the following to measure placental shape and structure:

1. 3D scans of the whole placenta.
2. 2D photographs of fetal surface and the sliced placental disk.
3. Histology samples of umbilical cord, extraplacental membranes and placental villous parenchyma.

To date, the placental materials include:

Total # of cases: 371

Total # of cases received 3D scans from: 261 (70%)

Total # of cases received fetal surface photos from: 290 (78%)

Total # of cases received maternal surface photos from: 290 (78%)

Total # of cases received slice photos from: 130 (35%)

Total # of cases received deformed due to fixation and storage: 333 (90%)

Total # of cases received that were not deformed due to fixation and storage: 38 (10%)

Total # of cases received without photographs: 16 (4%)

Total # of cases that arrived already cut (sliced/in pieces/bisected) and were photographed: 66 (18%)

Total # of cases received blocks from: 361 (97%)

Total # of blocks: 1,534

Of the total sample, 3D scans of the whole placenta have been obtained on 261 (70%). Of those for which scans were not obtained the reasons were as follows:

- 66 (60%) placentas previously dissected
- 28 (25%) placental deformation precluded scanning
- 16(15%) Other reasons: Cases received without photographs
-

Of the total sample, 2D digital photographs of the fetal and maternal surface have been obtained on 290 (78%). Of those for which fetal and maternal surface digital photographs were not obtained the reasons were as follows:

- 66 (81%) placentas previously dissected
- 15(19%) Other reasons: Cases received without photographs.
-

We anticipate the receipt of all study materials by the end of 2011.

Of note, the PI has also received 82 cases from the autism/ASD family study that is the EARLI network of Drs. Craig Newschaffer and Cheryl Walker. These cases represent placentas of infants born into families with an older sibling already diagnosed with autism/ASD. While these infants have of course not been diagnosed with autism/ASD, they do reflect the placental arborisation of families in which a tendency to the neuropathology that results in a diagnosis of autism/ASD has been made. As the oldest of these infants was born in late 2009, we anticipate that these children will begin to undergo tests germane to diagnoses of autism/ASD during the second year of this Innovative Idea Award and thus their placental samples can inform and extend the analyses of our principal ALSPAC cohort. Furthermore, these children have undergone extensive developmental testing at 6 and 12 months and so continuous measures of autism characteristics and precursors might also be examined prior to identification of cases.

To date, the placental materials from the autism/ASD family study of EARLI include:

Total # of EARLI cases: 82

Total # of cases received 3D scans from: 61 (74%)

Total # of cases received fetal surface photos from: 74 (90%)

Total # of cases received maternal surface photos from: 67 (82%)

Total # of cases received slice photos from: 74 (90%)

Total # of cases received blocks from: 66 (80%)

Total # of blocks: 601

Preliminary analyses from both these cohorts are presented below as appropriate.

SUBPROJECT 1: ANALYSIS OF 2-D CHORIONIC SURFACE VASCULATURE

P.I.: Carolyn M Salafia, MD, Institute for Basic Research (IBR), 1050 Forest Hill Road, Staten Island, NY, 10314.

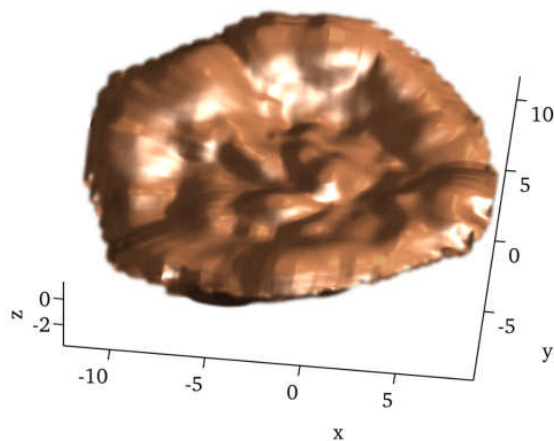
Co-Investigators: Michael Yampolsky, PhD, Department of Mathematics, University of Toronto, 105 George St, Toronto, ON M5A 2N4, Canada; Dawn P. Misra, PhD, Wayne State University, 3939 Woodward Avenue, Detroit, MI, 48201; Richard K. Miller, PhD, Department of Obstetrics and Gynecology, University of Rochester Medical Center (URMC), 601 Elmwood Avenue, Room 7-7550, Rochester, NY, 14642. (Note that there is use at any of the above addresses; use of archived anonymized digitized files only).

The chorionic surface vascular tree (laid down early in gestation, consistent with critical exposures periods for valproate and thalidomide on autism/ASD risk) will be extracted from the digital photographs of the chorionic surface.

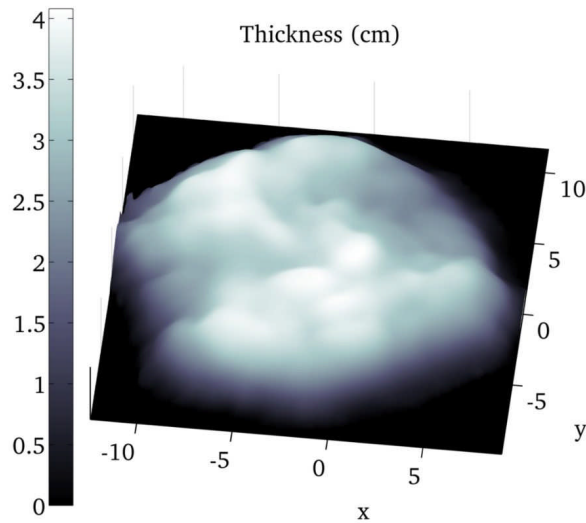
Status: Our original studies of the chorionic vasculature that laid the groundwork for the present proposal and methods involved the extraction of chorionic plate vasculature from 2D digital photographs of the fetal surface of the placenta. The chorionic plate digital photographs were obtained by well trained professionals in the University of Bristol Department of Pathology. As they were received by the PI, the chorionic plate digital photographs were screened for their suitability for chorionic plate analysis. Of 290 (78%) of placentas for which fetal chorionic plate photographs were obtained, 252 (87%) were deformed by fixation to a degree that precluded the extraction of physically meaningful measures of basic placental gross features such as chorionic plate perimeter, site of cord insertion relative to the chorionic plate edge, and chorionic plate vasculature. Therefore we have had to focus on extraction of these data from the 3D scans. After creating a 3D rendition of the placentas (a mesh), extraction of data requires gap filling in the mesh to create a closed solid from which volume and slice data can be extracted, and chorionic plate surface vessels are better perceived. We have developed improved methods for mesh rendering that have reduced analysis time and yielded improved reconstructions from which more and more precise shape and vascular structure data can be extracted.

A smoothed 3D placenta surface

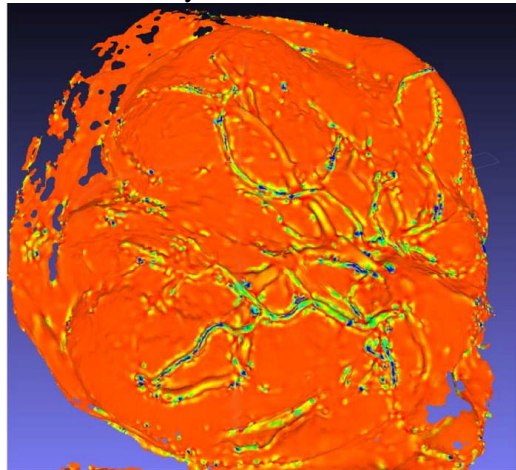
3D Placenta Surface



The thickness of the placenta, computed from the 3D surface. Notice that the thickness varies over space. The average thickness is 2.46cm and the standard deviation is 1.15cm.



Blood vessels identified by Gaussian curvature of the 3D surface.



Our protocol planned for the 2-D chorionic surface vascular trees to be transformed in a series of 2-D coordinates that represent points sampled along arbors (or paths) of chorionic vessels with the branching information. This skeletonization has already been accomplished, with the processing of those networks into a series of 2-D coordinates that represent points sampled along arbors (or paths) of chorionic vessels with the branching information. . The graph of a placenta's chorionic vasculature is obtained by computer analysis of an annotated image which determines the graph nodes from the labeled branch points and the graph edges based from the connecting vessel tracing lines. The result is a graph of the chorionic vasculature in an amenable format for further analysis, including vascular diameters, mean distances between branches which reflect cell division rates intervening between genetic triggering of vascular branching, etc. In addition, this allows more straightforward analysis of aspects of the branched networks of the chorionic vascular trees such as aspects of graph connectivity. (See Appendix for an example of a manually extracted vascular tree from a sample ALSPAC digital image of the fetal chorionic disk and for an example of its analysis and the resultant output skeletonization).

The resultant network can be analyzed as a structure the growth of which involved energy and entropy at specific different points along its evolution. An example of the thermodynamic entropy associated with different real placental trees is shown in the Appendix, with additional details regarding the physics.

Analysis of placental weight and beta, a measure of placental fractal growth

In a large population based birth cohort [1], we have previously established that human birth weight does not scale linearly with the weight of the placenta, but exhibits allometric scaling of $\frac{3}{4}$ power (a fractal dimension) consistent with Kleiber's Law for the basal metabolic rate. Allometric metabolic scaling [2] was first conjectured in the 1930s and has proved to be remarkably constant for a wide range of organisms from the smallest microbes ($\sim 10^{13}$ g) to the largest vertebrates and plants ($\sim 10^8$ g), [3] Placental branched growth is essentially fractal [4]. Using the Collaborative Perinatal Project, among women delivering after 34 weeks but prior to 43 weeks' gestation and with complete data for placental gross proportion measures (24,601 participants), the allometric metabolic equation was solved for β and β in regression of the dependence of placental weight on birth weight. Mean β was 0.78 ± 0.02 (range 0.66, 0.89), consistent with the 0.75 predicted by Kleiber's Law. In the context of our dynamical model of placental vascular growth [4], β relates the spatial shape of the placenta with the structure of the underlying vascular fractal. This dynamical empiric model recapitulates many of the known variant placental shapes (bilobate, multilobate, irregular or "scalloped") by a change of the fractal structure of the vasculature at a specific time instance. We have subsequently shown that deviations from space-filling symmetric fractal vascular growth are associated with histologically diagnosed vascular pathology and reduced placental vascular efficiency, that is, a smaller birth weight than predicted by the allometric scaling for the given placental weight [5] These findings are consistent with a connection between the allometric fetoplacental scaling and the fractal structure of the vascular supply system.

We have been able to analyse beta [β], in the ALSPAC group. As a first analysis, placental weight was compared in autism/ASD cases and controls. We found statistically significant differences overall in placental weight for cases of autism compared to normal controls only after stratifying on sex.

There was a statistically significant reduction in placental weight (~ 100 g) for female autism cases compared to female normal controls. This is true for the overall sample of females as well as when restricting the sample to children born at term gestation or adjusting for gestational age. This was not the result of outliers in either distribution. We did not find similar effects in males. While males represent the vast majority of autism cases, it appears that there may be differences within autism by sex.

The influence of gestational age on placental weight also appears to differ by sex. In multiple linear regression analyses predicting placental weight by case/control status and gestational age, we also saw that gestational age had a strong effect on placental weight for males but not for females.

There was no statistically significant difference in the larger placental dimension, smaller placental dimension, or in placental depth for autism cases compared to normal controls among males or females. However, the estimated difference among the girls was generally much larger than among the boys when comparing autism cases to controls. The difference in smaller placental dimension for autistic girls compared to normal control girls was the closest to being of statistical significance (-1.41 centimeters, $p=0.08$).

Based on these placental differences between males and females with diagnoses of autism/ASD, beta (β), a measure of placental functional efficiency calculated as \log placental weight/ \log birth weight, was calculated for the ALSPAC cohort. Beta did not differ between boys with autism/ASD (0.755 ± 0.0239) and those without such a diagnosis (0.753 ± 0.0202). However, β did differ between girls with autism/ASD (0.733 ± 0.0354) and those without such a diagnosis (0.760 ± 0.0161 , $P=0.001$). By contrast, β did differ by gestational age in boys (point estimate of effect= -0.002 , $p=0.009$). The association of altered β in girls with autism/ASD persisted after adjustment for gestational age (point estimate of effect of autism/ASD "case" status= 0.03 , $p=0.01$), and there was no independent effect of gestational age on β in girls ($p=0.53$).

| | Mean \pm sd | | Difference (autism vs. normal) | p-value |
|---|---------------------|---------------------|--------------------------------------|---------|
| | Autism cases | Normal controls | | |
| Placental weight (g) | | | | |
| <i>Overall</i> | 469.22 \pm 112.42 | 478.09 \pm 100.39 | -8.87 | 0.59 |
| <i>Males</i> | | | | |
| Unadjusted | 480.52 \pm 103.9 | 475.52 \pm 101.20 | +4.99 | 0.77 |
| Adjusted for gestational age | | | +3.86 | 0.81 |
| Term (\geq 37 weeks gestation) | | | +0.92 | 0.96 |
| <i>Females</i> | | | | |
| Unadjusted* | 395.00 \pm 145.23 | 495.10 \pm 95.40 | -100.10 | 0.045 |
| Adjusted for gestational age* | | | -99.62 | 0.050 |
| Term (\geq 37 weeks gestation)* | | | -100.10 | 0.045 |
| Larger placental dimension (cm) | | | | |
| Overall | 18.20 \pm 3.19 | 18.75 \pm 2.15 | -0.55 | 0.26 |
| Males | 18.28 \pm 3.00 | 18.80 \pm 2.26 | -0.52 | 0.29 |
| Females | 17.71 \pm 4.51 | 18.45 \pm 1.35 | -0.74 | 0.59 |
| Smaller placental dimension (cm) | | | | |
| <i>Overall</i> | 16.51 \pm 2.48 | 16.85 \pm 1.93 | -0.34 | 0.32 |
| <i>Males</i> | 16.74 \pm 2.50 | 16.92 \pm 1.97 | -0.18 | 0.63 |
| <i>Females</i> | 15.04 \pm 1.88 | 16.45 \pm 1.70 | -1.41 | 0.08 |
| Placental functional efficiency (β) | | | | |
| <i>Overall</i> | 0.7516 \pm 0.026 | 0.7539 \pm 0.019 | -0.0023 | 0.56 |
| <i>Males</i> | | | | |
| Unadjusted | 0.7545 \pm 0.024 | 0.7530 \pm 0.023 | +0.0016 | 0.67 |
| Adjusted for gestational age | | | +0.002 | 0.62 |
| <i>Females</i> | | | | |
| Unadjusted** | | | -0.0270 | 0.009 |
| Adjusted for gestational age** | 0.7333 \pm 0.035 | 0.7604 \pm 0.016 | -0.0270 | 0.010 |

Analysis of placental shape and cord insertion in a related cohort of familial autism, the EARLI cohort

We have also been able to utilize the EARLI placental materials in pilot analysis that will guide our analysis in the ALSPAC cohort. While some of the EARLI placentas shipped to the PI have been folded or become deformed in transport, we have 53 well preserved digital photographs of the fetal surface and 51 digital photographs of the sliced placental disk. These placentas have been processed identically to the University of North Carolina Pregnancy, Infection and Nutrition Study, extensively analysed by the PI [1, 2, 3, 5, 6] and are treated here as the reference group for the EARLI placentas.

In brief, umbilical cord marginality defined either by the first Fourier coefficient or more directly as the distance from the cord insertion to the disk edge differs significantly between autism/ASD cases and the UNC PIN birth cohort. Cord displacement is calculated as the displacement from the center of the area of the chorionic plate shape [7]; this displacement is greater in autism/ASD cases, meaning that cords are displaced closer to the placental chorionic disk margin. In addition, the disks of autism/ASD cases are less round, more irregular in perimeter, with significantly larger values of sigma and symmetric difference, measures of placental roundness, in autism/ASD cases (each $p < 0.0001$). Disk thickness in autism/ASD was also significantly less ($p < 0.0001$) as was the linear deviation from the average width (a measure of thickness variability, [2]). This finding was independent on the length of the slice (diameter of placental disk).

| | Mean \pm sd | | Difference (UNC vs. EARLI) | p- value |
|--|----------------------|-------------------------|-------------------------------|-------------|
| | UNC | EARLI | | |
| Fourier 1 | 3.231 \pm 1.817 | 4.069 \pm 2.345 | -.838 | .015 |
| Displacement | 3.455 \pm 1.911 | 4.228 \pm 2.515 | -.773 | .040 |
| Displacement/Diameter | .164 \pm .091 | .204 \pm .122 | -.040 | .029 |
| Sigma | 1.106 \pm .492 | 3.104 \pm 1.696 | -1.998 | .000 |
| Symmetric Difference | 138.815 \pm 67.609 | 3519.491 \pm 12086.36 | -220.676 | .000 |
| Average (Avg.) Width | 2.076 \pm .382 | 1.853 \pm .366 | .223 | .000 |
| Linear Deviation from Avg. Width | .340 \pm .111 | .368 \pm .148 | -.028 | .000 |
| Linear Deviation from Avg. Width Relative/Length | .020 \pm .007 | .019 \pm .008 | .001 | .005 |
| Average Width/Length | .125 \pm .029 | .100 \pm .035 | .025 | .110 |

Timeline: The final ALSPAC 3D scans and 2D digital photographs have been received within the last week. We will make rapid progress in these analyses since we have streamlined the programming that will not only increase efficiency but also improve precision.

Accomplishments for this Subproject

1. Analysis of the 2D digital image and 3D scan data, and the cohort medical data provided by ALSPAC has been implemented in this cohort. Improvements to image analysis algorithms have reduced analysis time and increased extractable data, and the precision of such data..
2. Additional autism/ASD cases from the EARLI project have been incorporated into this project at no additional cost.

SUBPROJECT 2: 3-D RECONSTRUCTION OF PLACENTAL VOLUME AS A PROXY FOR THE SHAPE OF THE CHORIONIC VASCULAR TREE

3D reconstructions of placental volume as a proxy for the shape of the chorionic vascular tree

Placental shapes, as captured in surface and slice images in the form of 3-D coordinate data, are created by rotating and translating the hand-traced 2D contours coordinates. Geometric descriptors will be easily extracted from the reconstructed shapes, such as surface area, volume, mean curvature, total curvature, shape moments, deviation from an average-shaped placenta, etc. These values will then be used in a classification approach, finding signatures for normal or abnormally shaped placentas, and to link these with our outcomes.

Chang [8] showed that 2D shape information of the placenta is meaningful for health prediction: "initial findings indicate significant relationships between shape of the placental surface and newborn's birth weight as well as their gestational age." Therefore, since 3D shape information is a superset of what is available in 2D, one would expect that health prediction based on 3D shape information would be even better, and is certainly merits investigation.

3-D reconstructions of finer placental branching vasculature *Sets of blocks obtained from placental parenchyma centered on a diving chorionic placental vessel will be serially sectioned as follows: Slides 1-3 H&E, 4-5 retained for possible future immunohistochemistry (IHC) stains, 6-8 stained with H&E, 9-10 retained unstained, etc.*

1. *The stained slides will be digitized and the series registered using standard registration techniques. Since villous branching is driven by vascular branching in the fetal systems, we need only to register the (larger) villus, simplifying the task of registration.*

2. *The registered 3-D structure will be pruned of the terminal villi, development of which is by simple capillary extension and therefore do not reflect the mechanism of growth we are targeting. This radically simplifies the fine chorionic vascular tree.*
3. *These 3-D networks will be transformed and analyzed as in Subproject 1, above.*

Status: We have explored many methods for color image segmentation. This problem is difficult for several reasons:

- color variation from uneven staining prevents a simple uniform threshold
- aging of stain makes the color different, require adaptive strategy
- thin tissue causes nearly transparent color
- thick tissue cause dark color and out of focus

The basic principle that we use for segmentation is that the slide background is white. Thus an approach is to determine for every pixel a scalar quantity describing how white that pixel is, and then comparing this quantity to a threshold. The details then are in how to compute the scalar quantity and how to set the threshold. For different applications and purposes, we adapt suitable thresholds and quantity for the specific characteristics, for example, the non-white staining cells in muscle tissue and Wharton's jelly appear different.

We have considered a number of mathematical methods for tissue/background segmentation:

1. Threshold on statistics of different color channels (RGB to Lab)

To adapt to color variations in stain, we set the threshold in a data-dependent manner. We have investigated segmentation schemes where the threshold is set according to statistics of the red, green and blue color channels (as well as statistics of color components in other color representations, such as hue, saturation, and value).

2. K-mean clustering of the colors

K-means is a generic method for clustering. To apply it, we first pick references for the colors that we wish to distinguish (red tissue, blue nuclei, and white background), then we categorize every pixel in the image into one color based on the nearest neighbor distance. By iterating the references in every loop, we get better cluster centers for red, blue and white. As a result, comparing all the pixels to them, we can mark all the pixels to the correct color.

3. C-means (fuzzy K-means)

Fuzzy logic is very useful in our applications. Due to the natural overlap in tissue and cell as well as artifacts introduced by sampling and digitization, color does not appear clean, especially at the boundary of cells. To overcome this problem, we apply the fuzzy logic theory, in which give freedom to ambiguity pixels freedom to be red or blue or both. As long as the majority of color segmentation is correct, the application of fuzzy logic in our method can prevent the few strange pixels from compromising the accuracy of the segmentation.

4. One-dimensional colormap created by neural network optimization

In [9], the authors propose a method to normalize colors by building a color map that is adapted to the image, a kind of neural network called a self-organizing map (SOM). A SOM network is effectively a kind of regression: under a smoothness condition, it finds the best curve that fits the input data. Here, the data is the set of color pixels of the image. In our example, a colormap is found using the SOM method. The image is then converted to an indexed image by assigning each pixel the closest color in the SOM colormap. We can segment the image by simple thresholding applied to the indices. See the Appendix for an example of an image segmented into nuclei (blue), tissue (red), and gap (white).

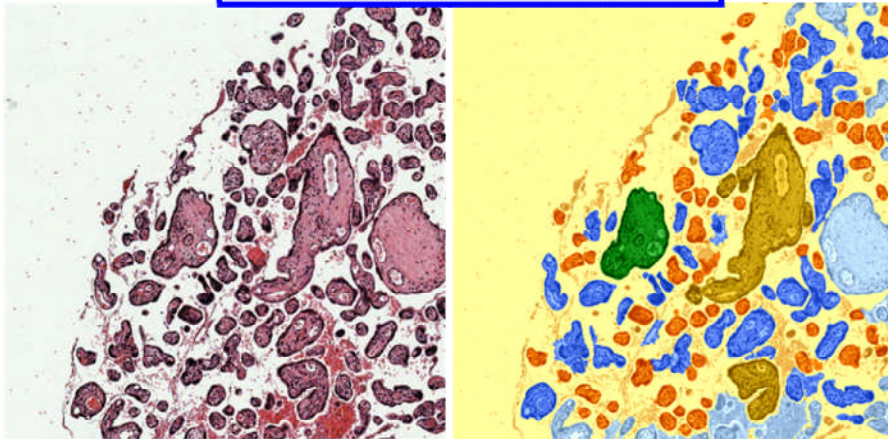
5. Looking at morphological connectivity of segments

For specific cell type detection, first a color-based segmentation strategy can separate blue and red, which is a way to separate the cells and background. However, two types of cells may have nuclei that appear blue and resemble in a round shape too. This mean that any local color based method cannot work effectively here to distinguish them.

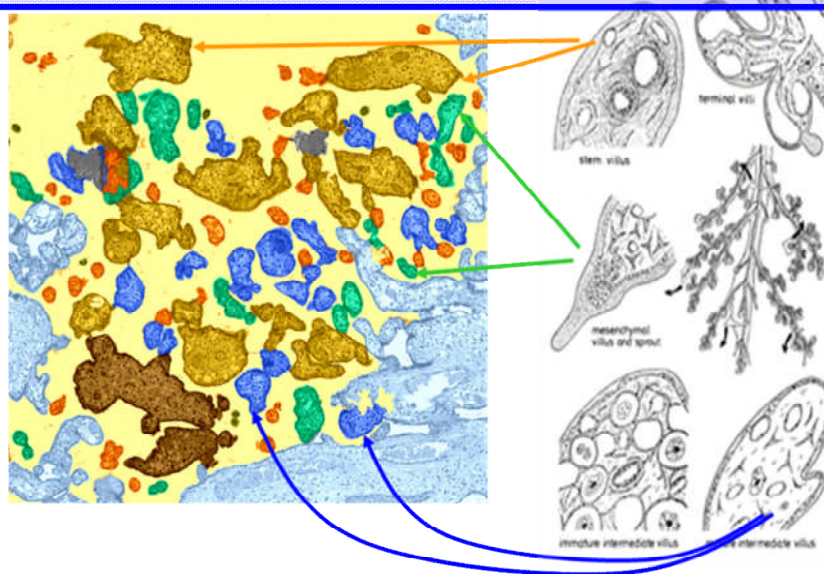
However, none of the above methods have demonstrated the ability to retain the “meaning” of the segmented object as our initial work with Definiens (2008). This work is the basis for our present approach. Seven “gold standard” hematoxylin and eosin stained samples of placental villous branching morphogenesis types provided by Dr. Peter Kaufmann, renowned placental morphologist. 80 variables were analyzed and reduced to 9 factors using principal components factor analysis (PCA). The 6

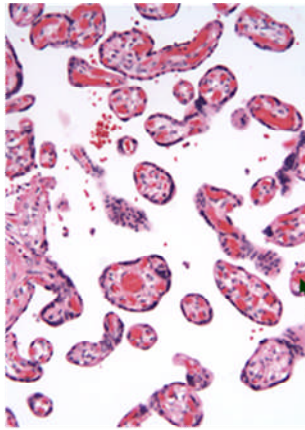
paradigm patterns of abnormal placental villous branching were distinguishable from “term normal” by ≥ 1 factors, suggesting our approach was tenable. Beyond simply segmenting the image, we attempt to determine the higher-level “meaning” of the segmented objects from its morphological descriptors of the component shape (e.g., area) and statistics of the image within the component (e.g., average red intensity). However, we have not been as successful in this aspect as in our initial work with Definiens.

Raw and segmented images

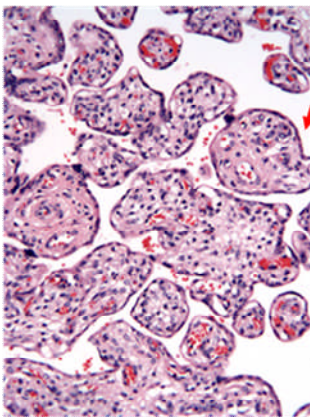


Correlation of segmented image with villous types

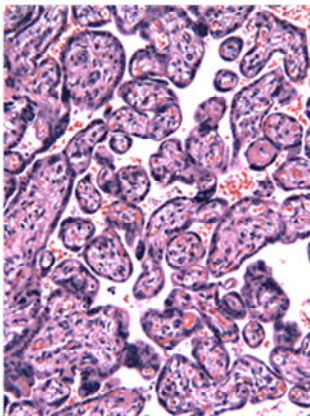




Factor 2: “(-)”



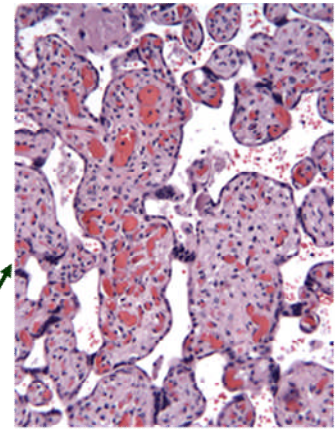
Factor 3: “(-)”



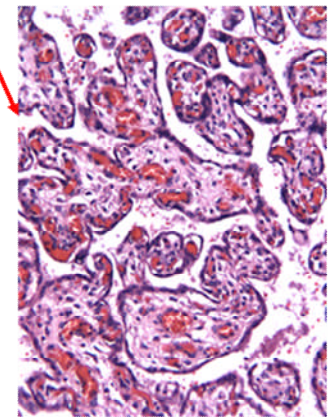
Factor 5: “(-)”

Table of correlations of factor scores with birthweight, gestational age and placental weight.

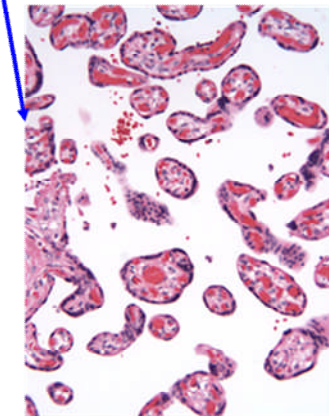
| | | Birth weight | Gestational age | Placental weight |
|-----------|---------|------------------|-----------------|------------------|
| Factor 1 | R | .013 | .087 | -.084 |
| | P value | NS | NS | NS |
| Factor 2 | R | .217(**) | .148(*) | .034 |
| | P value | .001 | .020 | .606 |
| Factor 3 | R | .346(**) | .153(*) | -.046 |
| | P value | .000 | .016 | .458 |
| Factor 4 | R | -.003 | -.007 | .026 |
| | P value | NS | NS | NS |
| Factor 5 | R | .018 | -.053 | .137(*) |
| | P value | NS | NS | .030 |
| Factor 6 | R | -.082 | -.115 | .086 |
| | P value | NS | .072 | NS |
| Factor 7 | R | -.165(**) | -.083 | .050 |
| | P value | .009 | NS | NS |
| Factor 8 | R | -.167(**) | -.136(*) | -.118 |
| | P value | .009 | .033 | .065 |
| Factor 9 | R | .044 | .008 | -.011 |
| | P value | NS | NS | NS |
| Factor 10 | R | .028 | .022 | .121 |
| | P value | NS | NS | .059 |
| Factor 11 | R | .098 | .140(*) | -.074 |
| | P value | NS | .028 | NS |
| Factor 12 | R | -.003 | .088 | -.188(**) |
| | P value | NS | NS | .003 |
| Factor 13 | R | .138(*) | .064 | .232(**) |
| | P value | .030 | .314 | .000 |
| Factor 14 | R | .117 | .040 | -.124 |
| | P value | .066 | NS | .052 |
| Factor 15 | R | .034 | -.068 | .131(*) |
| | P value | NS | NS | .040 |
| Factor 16 | R | .079 | .083 | -.052 |
| | P value | NS | NS | NS |



Factor 2: “(+)”



Factor 3: “(+)”



Factor 5: “(+)”

** Correlation is significant at the 0.01 level (2-tailed).
* Correlation is significant at the 0.05 level (2-tailed).

Factors are mathematical constructs that are difficult to characterize on inspection of the factor loadings of the individual histology item measures. The first 5 factors accounted for 67% of the total data variance. We calculated factors scores for each case, and selected photomicrographs from cases with extreme low (“negative”) and high (“positive”) factor scores. However, histologically, factors appear to mark visually distinct patterns of villous sizes, stromal composition, trophoblast features and capillary architecture.

| Component | Initial Eigenvalues | | |
|------------------|----------------------------|----------------------|---------------------|
| | Total | % of Variance | Cumulative % |
| Factor 1 | 40.584 | 36.56 | 36.56 |
| Factor 2 | 11.518 | 10.38 | 46.94 |
| Factor 3 | 9.296 | 8.38 | 55.31 |
| Factor 4 | 7.386 | 6.65 | 61.97 |
| Factor 5 | 4.954 | 4.46 | 66.43 |
| Factor 6 | 4.293 | 3.87 | 70.30 |
| Factor 7 | 3.601 | 3.24 | 73.54 |
| Factor 8 | 3.190 | 2.87 | 76.42 |
| Factor 9 | 2.700 | 2.43 | 78.85 |
| Factor 10 | 1.841 | 1.66 | 80.51 |
| Factor 11 | 1.709 | 1.54 | 82.05 |
| Factor 12 | 1.551 | 1.40 | 83.45 |
| Factor 13 | 1.457 | 1.31 | 84.76 |
| Factor 14 | 1.251 | 1.13 | 85.89 |
| Factor 15 | 1.172 | 1.06 | 86.94 |
| Factor 16 | 1.114 | 1.00 | 87.95 |

***SUBPROJECT 3: EPIDEMIOLOGY OF GESTATIONAL MODIFIERS OF PLACENTAL
VASCULAR STRUCTURE AND ASD RISK***

P.I: W. Ted Brown, MD, PhD, IBR; Co-Investigators: Carolyn M Salafia, MD, IBR; Eric London, MD, IBR; Dawn P. Misra, PhD, Department of Family Medicine and Public Health Services, Wayne State University School of Medicine, 101 E. Alexandrine, Room #203, Detroit, MI, 48201 (no animal or human use at any of the above addresses; use of archived anonymized data only).

This is a Year 2 operation.

KEY RESEACH ACCOMPLISHMENTS

This project has been proceeding well. The acquisition of images from placentas preserved in the ALSPAC archive has been completed. Images and data from the EARLI project have been incorporated into this project and have informed both the analytical techniques as well as the understanding of the results of this project. We have been able to utilize the EARLI placental materials in pilot analysis that will guide our analysis in the ALSPAC cohort. What we glean from these analyses are also being applied to the National Children's Study to further improve that study's effectiveness, and the power of a predictive tool for autism/ASD risk assessment from placental measures.

The analyses of 2D and 3D images from this project are in process. We have identified and resolved a number of issues regarding algorithm programming. Improvements in the image analysis algorithms are speeding the image processing rate.

1. The 371 placentas from the ALSPAC archive have been selected, photographed, scanned using the 3D scanner, and dissected per the project schedule.
2. Analysis of the 2D and 3D digital image data and the cohort data provided by ALSPAC has been implemented successfully. Improvements to the image analysis algorithms have reduced analysis time.
3. Additional autism/ASD cases from the EARLI project have been incorporated into this project at no additional cost.

REPORTABLE OUTCOMES

An abstract of these results is being prepared for presentation at the Society for Gynecological Investigation (SGI) meeting in March 2012.

1. There was a statistically significant reduction in placental weight (~100 g) for female autism cases compared to female normal controls. This is true for the overall sample of females as well as when restricting the sample to children born at term gestation or adjusting for gestational age. This was not the result of outliers in either distribution. We did not find similar effects in males. While males represent the vast majority of autism cases, it appears that there may be differences within autism by sex.
2. The influence of gestational age on placental weight also appears to differ by sex. In multiple linear regression analyses predicting placental weight by case/control status and gestational age, we also saw that gestational age had a strong effect on placental weight for males but not for females.
3. There was no statistically significant difference in the smaller placental dimension for autism cases compared to normal controls among males or females. However, the estimated difference among the girls (~0.82 cm) was approximately two times larger than among the boys (~0.43 cm)
4. Based on these placental differences between males and females with diagnoses of autism/ASD, β , a marker of placental functional efficiency as well as placental fractal structure, was calculated for the ALSPAC cohort. Beta did not differ between boys with autism/ASD (0.755 ± 0.0239) and those without such a diagnosis (0.753 ± 0.0202). However β did differ between girls with autism/ASD (0.733 ± 0.0354) and those without such a diagnosis (0.760 ± 0.0161 , $P=0.001$). By contrast, β did differ by gestational age in boys (point estimate of effect = -0.002, $p=0.009$). The association of altered β in girls with autism/ASD persisted after adjustment for gestational age (point estimate of effect of autism/ASD "case" status = 0.03, $p=0.01$), and there was no independent effect of gestational age on β in girls ($p=0.53$).

CONCLUSIONS

To date, the study is progressing well. We have extracted from a large archive of a well known and intellectually productive birth cohort a set of specimens that have never before been studied by the ALSPAC team or any collaborators. This placenta sample represents the largest collection of placentas from a population cohort in which neurodevelopmental examinations were universally applied and placentas were archived. Thus we not only have an unbiased placental sample of a population of cases of autism/ASD, but also of control children with special education needs and controls with normal neurodevelopment. In addition, the growing cohort of high-autism-risk families (EARLI), families with an autistic older sibling and a new pregnancy, is providing a second group that can extend, focus and validate our analyses in the coming year.

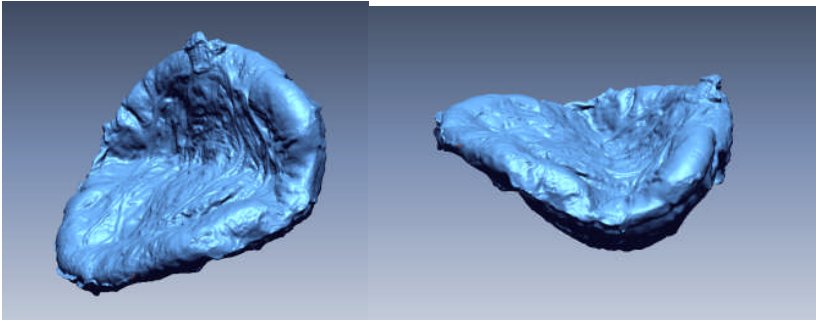
Most importantly, our preliminary analyses confirm our hypothesis that placental structure, even as measured by our relatively crude first year measures, varies between autism/ASD cases, and in families with an autistic sibling, compared to a large birth cohort.

REFERENCES

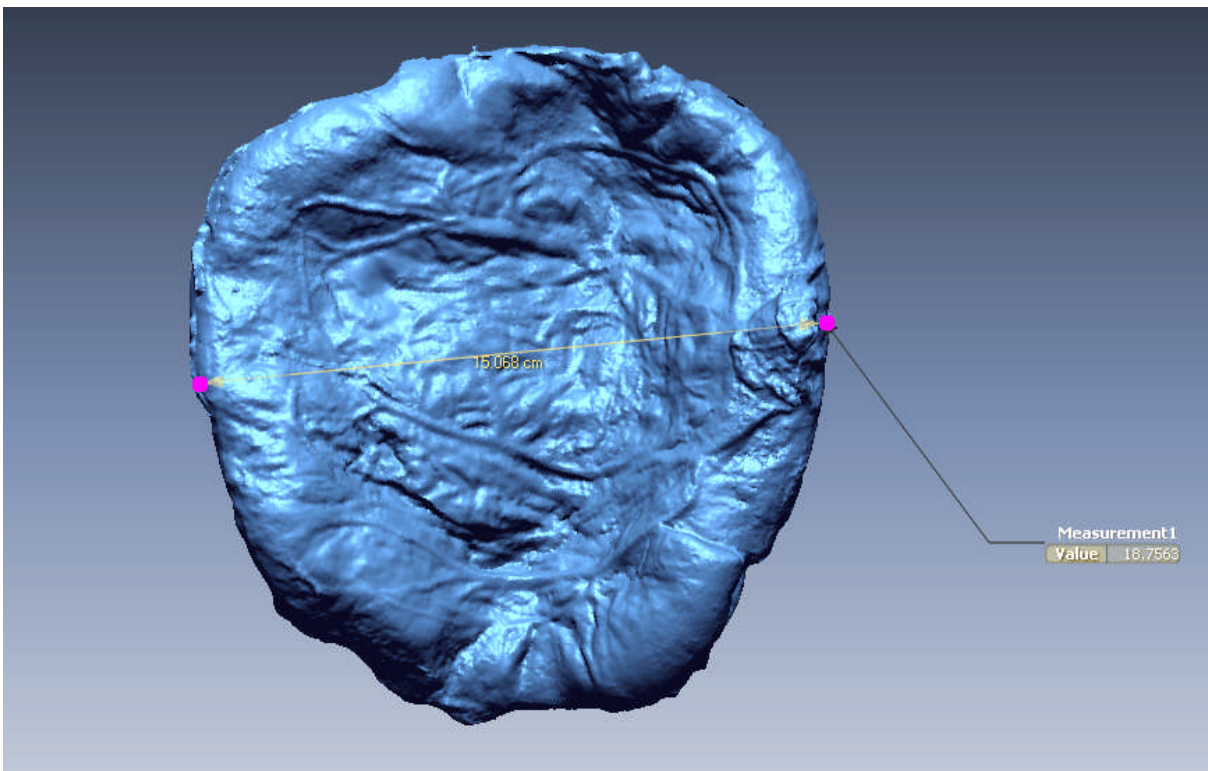
1. Niswander K, Gordon M. The Collaborative Perinatal Study of the National Institute of Neurological Diseases and Stroke: the Women and Their Pregnancies. Philadelphia, PA: W.B. Saunders, 1972.
2. Kleiber M. The Fire of Life. Revised ed. s.l. Robert E. Krieger Publ. Co.; 1975.
3. Baker AM, Braun JM, Salafia CM, Herring AH, Daniels J, Rankins N, Thorp JM. Risk factors for uteroplacental vascular compromise and inflammation. *Am J Obstet Gynecol*. 2008 Sep; 199(3):256.e1-9.
4. James GBW, Brown H, editors. *Scaling in Biology*. Santa Fe Institute studies in the sciences of complexity proceedings. New York, NY: Oxford University Press; 2000. p. 368.
5. Yampolsky M, Salafia CM, Shlakter O, Haas D, Eucker B, Thorp JM. Modeling the variability of shapes of a human placenta. *Placenta* 2008;29(9): 790–7
6. Salafia CM, Maas E, Thorp JM, Eucker B, Pezzullo JC, Savitz DA. Measures of placental growth in relation to birth weight and gestational age. *Am J Epidemiol*. 2005 Nov 15; 162(10):991-8.
7. Yampolsky M, Salafia CM, Shlakter O, Haas D, Eucker B, Thorp J. Centrality of the Umbilical Cord Insertion in a Human Placenta Influences the Placental Efficiency. *Placenta*. 2009 30(12):1058-64.
8. Jen-Mei Chang, Amy Mulgew, Carolyn Salafia, A Geometric Approach to Study the Relationship between Maternal and Fetal Characteristics and Shape of Placental Surfaces, under review.
9. Sertel, Kong, Catalyurek, Lozanski, Saltz, Gurcan. Histopathological Image Analysis Using Model-Based Intermediate Representations and Color Texture: Follicular Lymphoma Grading. *JSign Process Syst*, 2008.

APPENDIX

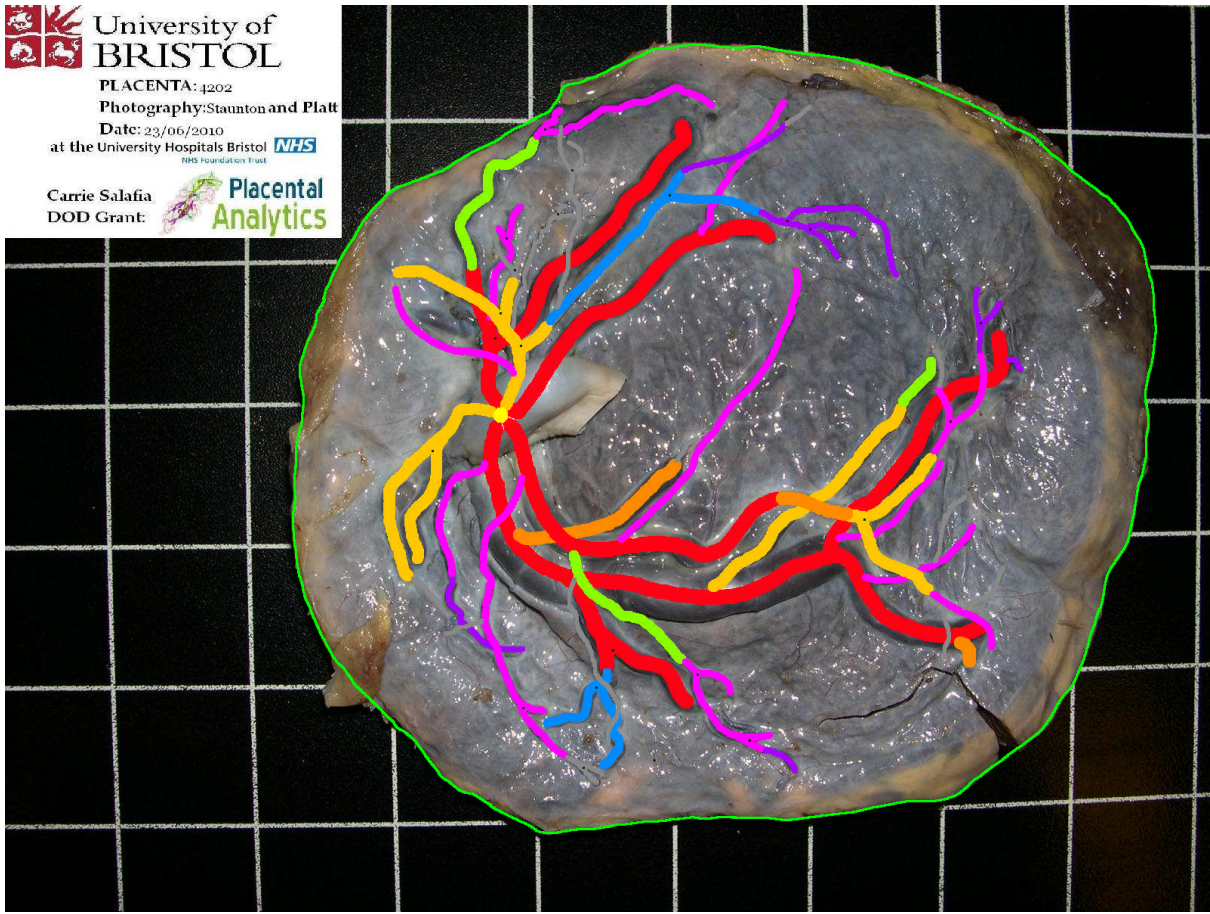
2D photograph of a placenta



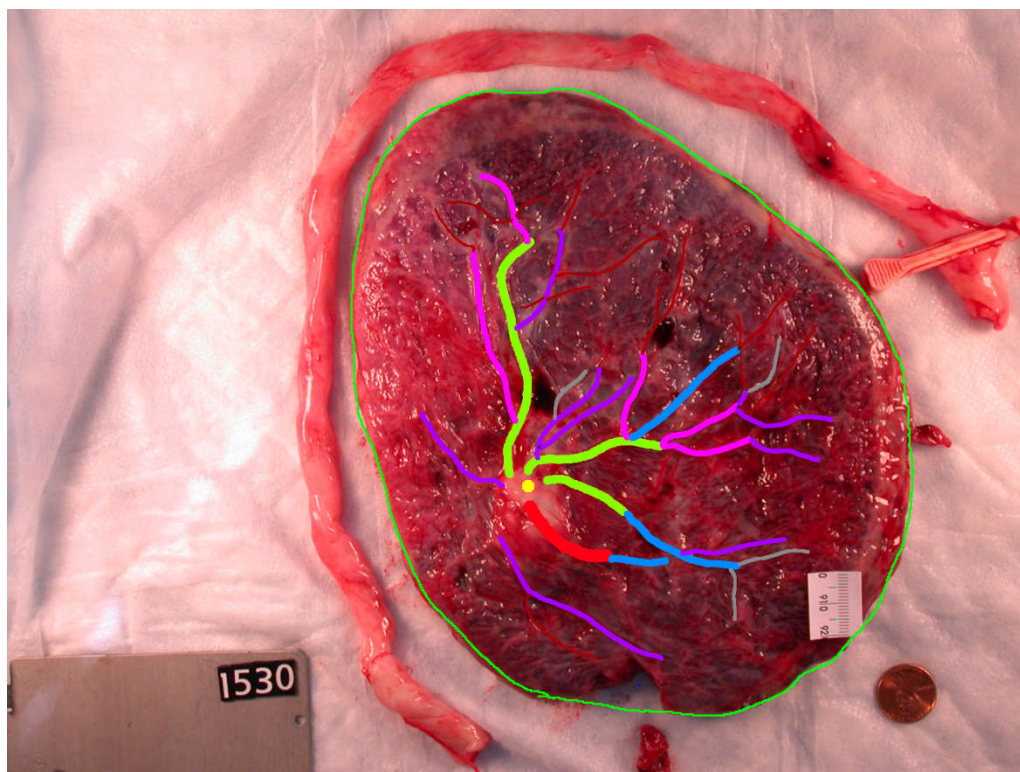
Images of the placenta mesh formed from the 3D scans



The measurement of 15.068 cm is the linear distance between the two pink points; it is the distance we would get if we only considered the 2D photo. Measurement 1 Value 19.834 is the actual distance (the geodesic distance) measured on the placenta between the two pink points. This highlights the issue of dealing with 2D photographs of deformed placentas - we cannot use the 2D photos and expect to get correct data.



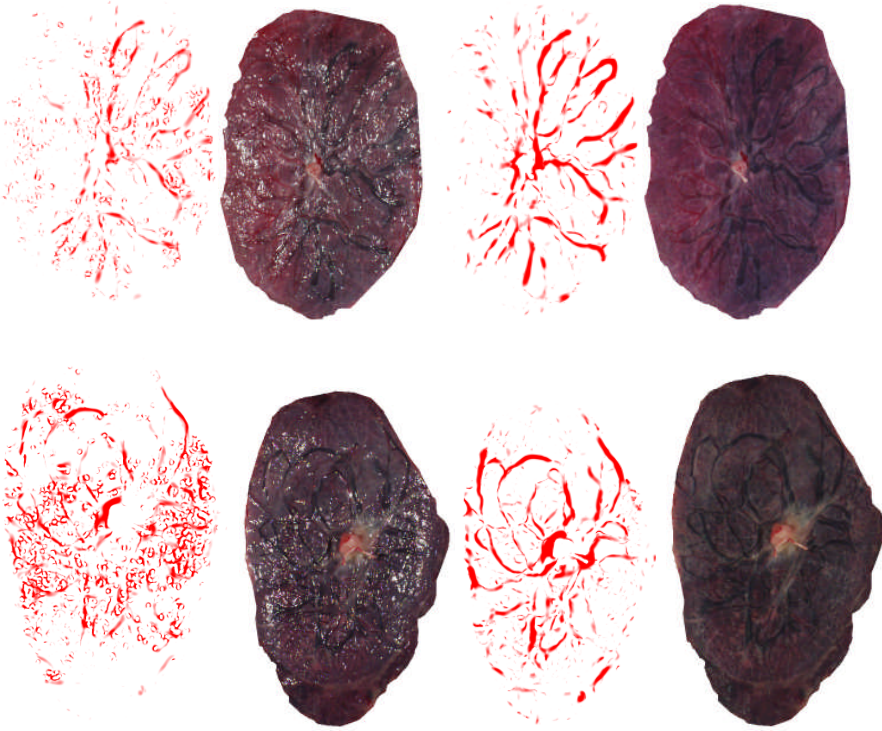
The vascular tracing of a 2D photograph of the fetal surface of ALSPAC placenta



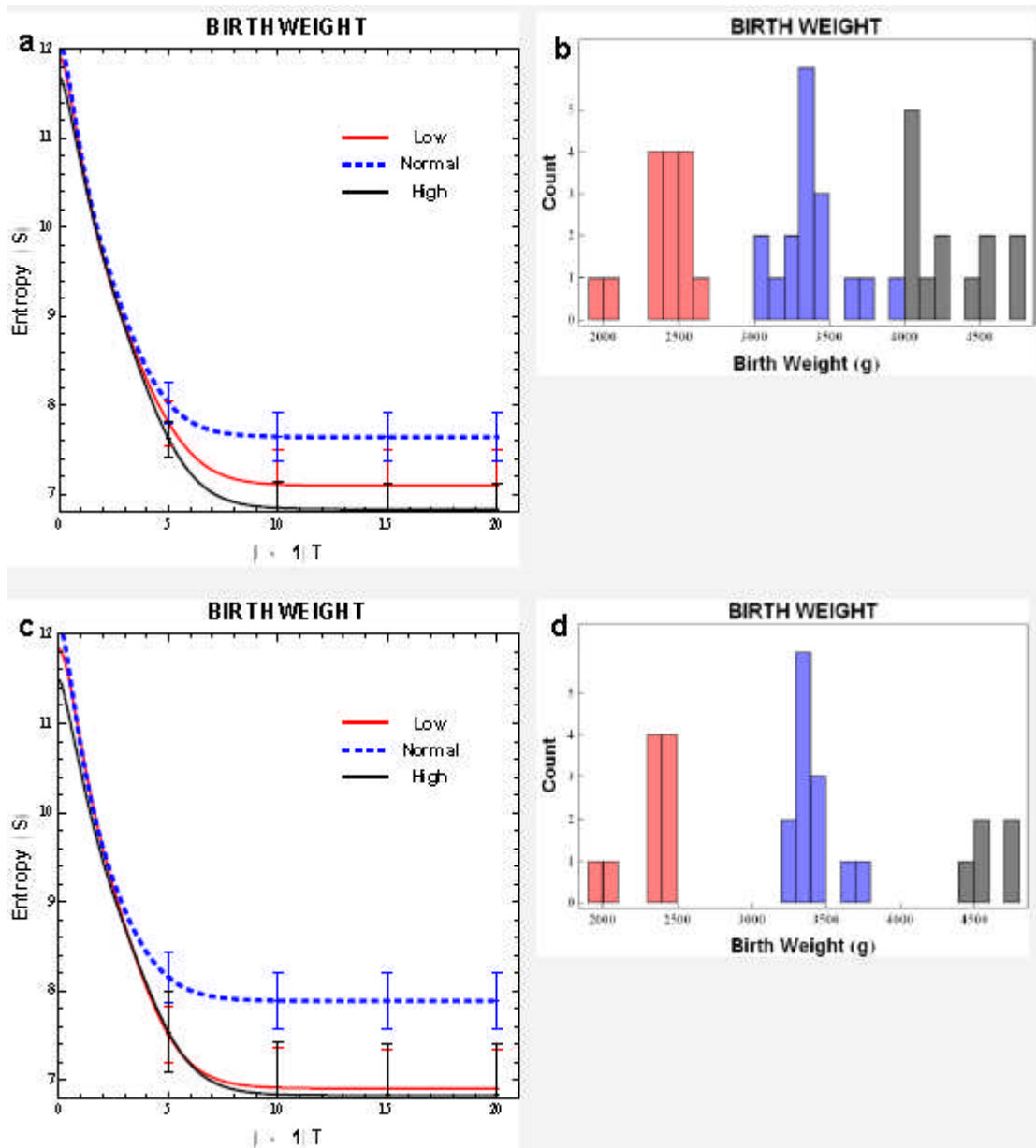
Output:

Coordinates of connectivity points

| | X | Y | Input Diameter | Output Diameter |
|----|------|-----|----------------|-----------------|-----------------|-----------------|-----------------|-----------------|
| 0 | 1017 | 518 | 13 | 9 | 11 | 0 | 0 | 0 |
| 1 | 1139 | 578 | 11 | 7 | 9 | 0 | 0 | 0 |
| 2 | 1154 | 601 | 9 | 5 | 3 | 0 | 0 | 0 |
| 3 | 1023 | 183 | 7 | 3 | 0 | 0 | 0 | 0 |
| 4 | 1135 | 246 | 5 | 3 | 0 | 0 | 0 | 0 |
| 5 | 817 | 286 | 7 | 3 | 0 | 0 | 0 | 0 |
| 6 | 1134 | 325 | 11 | 5 | 0 | 0 | 0 | 0 |
| 7 | 1141 | 330 | 11 | 5 | 0 | 0 | 0 | 0 |
| 8 | 1032 | 334 | 11 | 3 | 0 | 0 | 0 | 0 |
| 9 | 939 | 338 | 19 | 11 | 0 | 0 | 0 | 0 |
| 10 | 1052 | 346 | 11 | 7 | 0 | 0 | 0 | 0 |
| 11 | 1251 | 351 | 5 | 3 | 0 | 0 | 0 | 0 |
| 12 | 1215 | 369 | 7 | 3 | 0 | 0 | 0 | 0 |
| 13 | 963 | 409 | 13 | 11 | 0 | 0 | 0 | 0 |
| 14 | 775 | 450 | 9 | 7 | 0 | 0 | 0 | 0 |
| 15 | 1268 | 493 | 7 | 3 | 0 | 0 | 0 | 0 |
| 16 | 826 | 494 | 13 | 9 | 0 | 0 | 0 | 0 |
| 17 | 832 | 510 | 9 | 7 | 0 | 0 | 0 | 0 |
| 18 | 1159 | 523 | 9 | 7 | 0 | 0 | 0 | 0 |
| 19 | 973 | 525 | 13 | 11 | 0 | 0 | 0 | 0 |
| 20 | 965 | 526 | 13 | 9 | 0 | 0 | 0 | 0 |
| 21 | 791 | 552 | 13 | 9 | 0 | 0 | 0 | 0 |
| 22 | 853 | 558 | 9 | 5 | 0 | 0 | 0 | 0 |

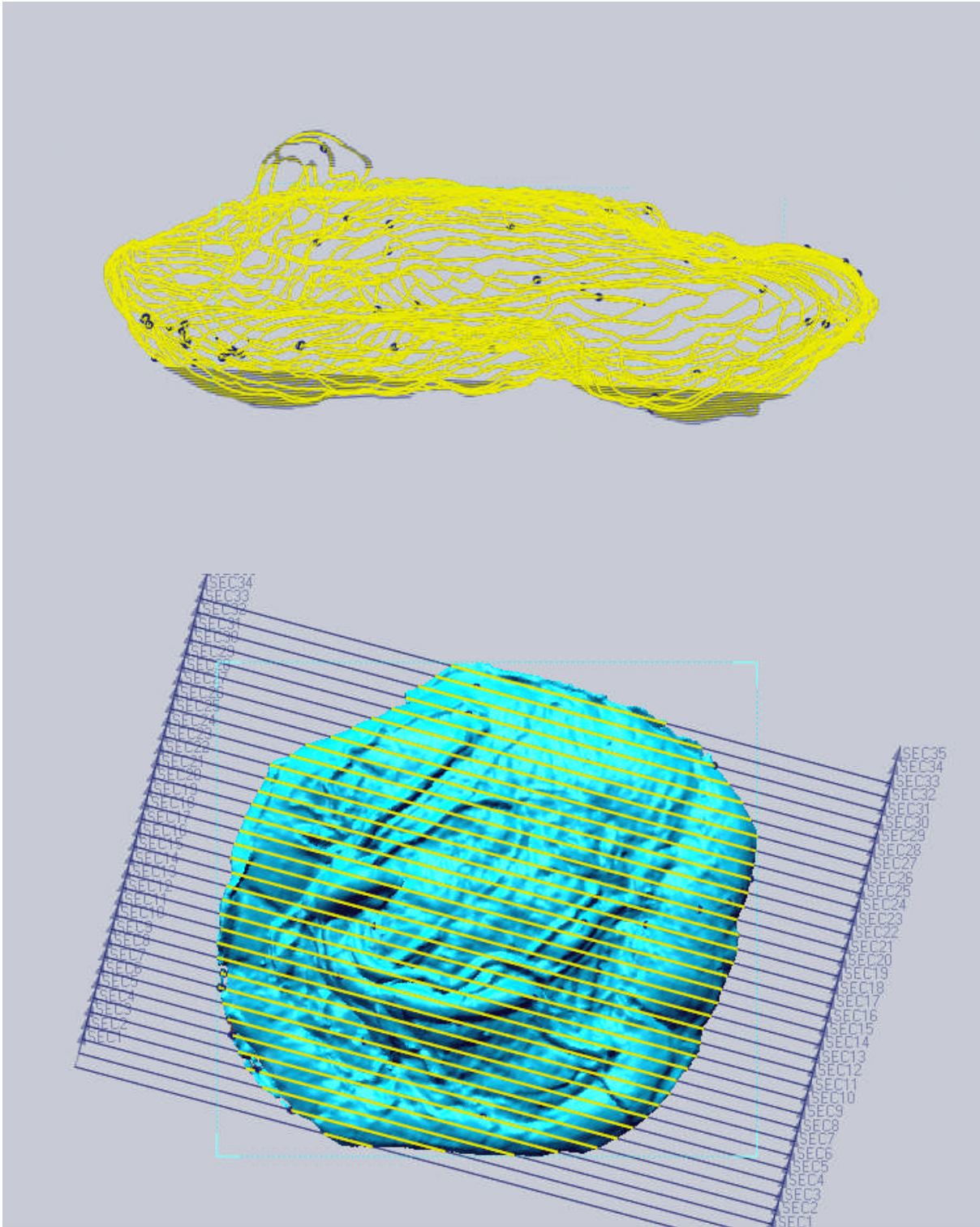


Photographs with and without filter comparison. Frangi vesselness method is applied to two placenta images.

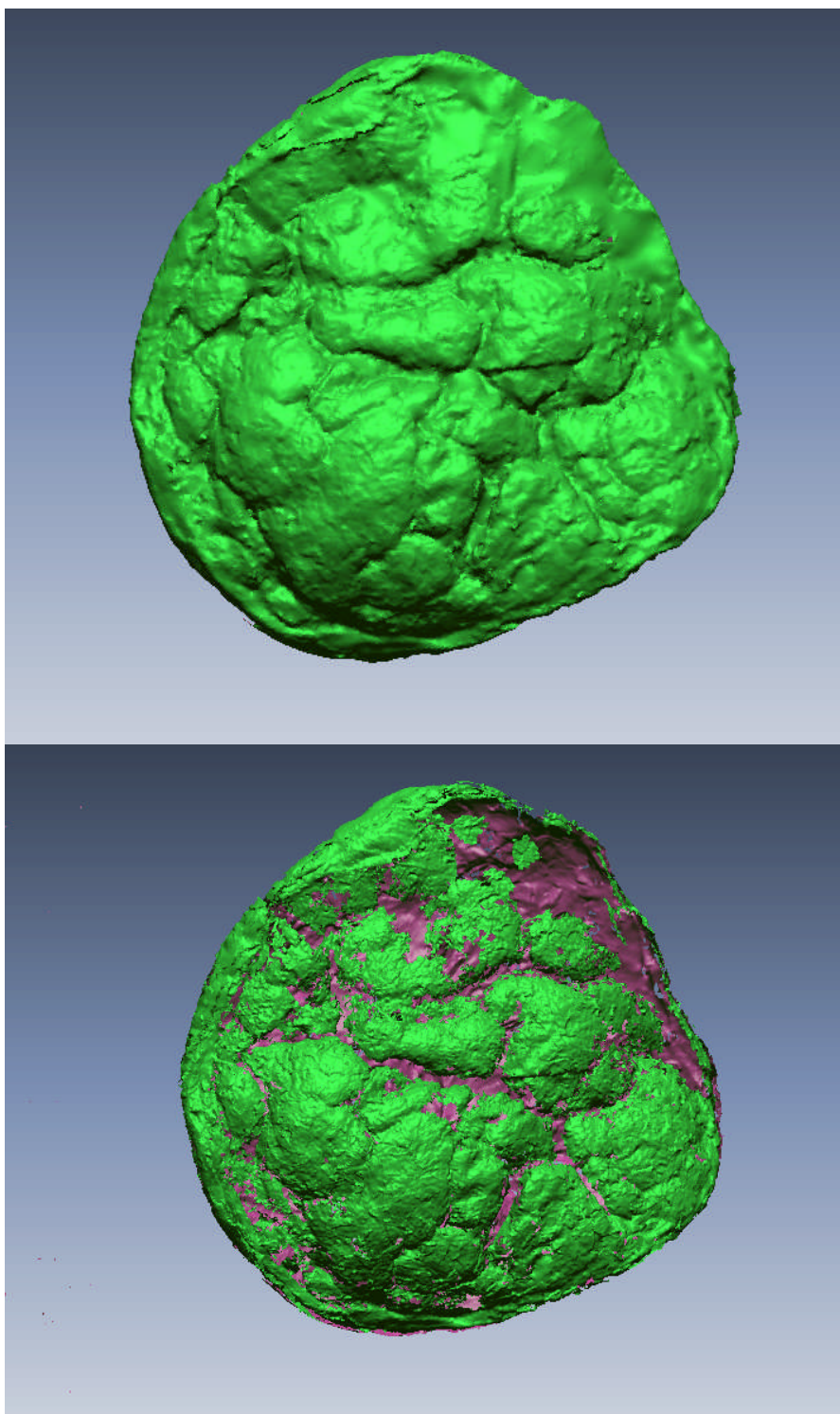


The vasculature and its branching points are represented by edges and vertices respectively. An edge connects a n th generation vertex to a $(n+1)$ th generation vertex. Two edges are sides of a triangle if its corners are a n th generation vertex and two $(n+1)$ th generation vertices. A function called the entropy (S) is introduced to measure the distribution of triangle areas in the tree. A high area distribution relates to a higher symmetry in the branching structure. By varying the distribution parameter β , one is able to weight generations of the network differently.

Panel (a) shows the means of the area distribution functions for 45 placentas divided into sets corresponding to low, normal and high birth weights of the baby. Panel (c) shows the means of the area distribution functions for 28 placentas divided into more constrained sets. Panels (b) and (d) show the corresponding distributions of the birth weights in the chosen placenta sample. Panels (a) and (c) indicate that the distribution of triangle areas and hence the branching symmetry in a normal birth weight placenta is higher closer to the umbilical cord insertion point (large β) than for the abnormal cases. The area distributions of all three types of placenta converge by moving away from the umbilical cord insertion point (small β).



Snapshots that capture the slices of a 3D image made with rapidform



TOP: The maternal surface of a placenta formed from 3Dscans with initial methods.

BOTTOM: The maternal surface of the same placenta formed from 3D scans using our current methods of mesh refining.